SLC39A14 deficiency alters manganese homeostasis and excretion resulting in brain manganese accumulation and motor deficits in mice

Supak Jenkitkasemwong[a], Adenike Akinyode[a], Elizabeth Paulus[a], Ralf Weiskirchen[b], Shintaro Hojyo[c], Toshiyuki Fukada[d,e,f], Genesys Giraldo[g,h], Jessica Schrier[g,h], Armin Garcia[g,h], Christopher Janus[g,h], Benoit Giasson[g,h], and Mitchell D. Knutson[a,1]

[a]Food Science & Human Nutrition Department, University of Florida, Gainesville, FL 32611; [b]Institute of Molecular Pathobiochemistry, Experimental Gene Therapy and Clinical Chemistry, University Hospital Rheinisch-Westfälische Technische Hochschule Aachen, D-52074 Aachen, Germany; [c]Osteoimmunology, Deutsches Rheuma-Forschungszentrum Berlin, 10117 Berlin, Germany; [d]Molecular and Cellular Physiology, Faculty of Pharmaceutical Sciences, Tokushima Bunri University, Tokushima 770-8514, Japan; [e]Division of Pathology, Department of Oral Diagnostic Sciences, School of Dentistry, Showa University, Shinagawa 142-8666, Japan; [f]RIKEN Center for Integrative Medical Sciences, Yokohama 230-0045, Japan; [g]Department of Neuroscience, College of Medicine University of Florida, Gainesville, FL 32611; and [h]Center for Translational Research in Neurodegenerative Disease, College of Medicine University of Florida, Gainesville, FL 32611

Edited by Valeria Cizewski Culotta, Johns Hopkins University, Baltimore, MD, and accepted by Editorial Board Member Michael A. Marletta January 12, 2018 (received for review November 29, 2017)

Solute carrier family 39, member 14 (SLC39A14) is a transmembrane transporter that can mediate the cellular uptake of zinc, iron, and manganese (Mn). Studies of *Slc39a14* knockout (*Slc39a14*$^{-/-}$) mice have documented that SLC39A14 is required for systemic growth, hepatic zinc uptake during inflammation, and iron loading of the liver in iron overload. The normal physiological roles of SLC39A14, however, remain incompletely characterized. Here, we report that *Slc39a14*$^{-/-}$ mice spontaneously display dramatic alterations in tissue Mn concentrations, suggesting that Mn is a main physiological substrate for SLC39A14. Specifically, *Slc39a14*$^{-/-}$ mice have abnormally low Mn levels in the liver coupled with markedly elevated Mn concentrations in blood and most other organs, especially the brain and bone. Radiotracer studies using ^{54}Mn reveal that *Slc39a14*$^{-/-}$ mice have impaired Mn uptake by the liver and pancreas and reduced gastrointestinal Mn excretion. In the brain of *Slc39a14*$^{-/-}$ mice, Mn accumulated in the pons and basal ganglia, including the globus pallidus, a region susceptible to Mn-related neurotoxicity. Brain Mn accumulation in *Slc39a14*$^{-/-}$ mice was associated with locomotor impairments, as assessed by various behavioral tests. Although a low-Mn diet started at weaning was able to reverse brain Mn accumulation in *Slc39a14*$^{-/-}$ mice, it did not correct their motor deficits. We conclude that SLC39A14 is essential for efficient Mn uptake by the liver and pancreas, and its deficiency results in impaired Mn excretion and accumulation of the metal in other tissues. The inability of Mn depletion to correct the motor deficits in *Slc39a14*$^{-/-}$ mice suggests that the motor impairments represent lasting effects of early-life Mn exposure.

SLC39A14 | manganese | liver | pancreas

Manganese (Mn) is an essential trace mineral required for normal growth and physiological processes, such as bone formation, immune response, and carbohydrate metabolism (1). The essentiality of Mn derives from its role as a cofactor in a variety of enzymes, including galactosyl transferase, Mn-superoxide dismutase, xanthine oxidase, arginase and glutamine synthetase, and pyruvate decarboxylase.

The total amount of Mn in the human body is ∼10–20 mg, with the highest concentrations found in the liver, pancreas, and kidney (2). The bone appears to be a major storage site, accounting for nearly 40% of total body Mn (3). Daily intakes of Mn typically range from 2 to 6 mg, of which ∼1–5% is normally absorbed (4). Mn is abundant in plant-based foods, whereas animal foods, including meat, fish, poultry, eggs, and dairy, are nearly devoid of this metal. Significant sources of Mn in typical diets include whole grains, rice, nuts, beans, and leafy vegetables. In the United States, the adequate intake for Mn is 2.3 mg/d and 1.8 mg/d for adult men and women, respectively.

While naturally occurring dietary Mn deficiency has not been reported, Mn excess and toxicity have been well described, as exposure to high levels of the metal can lead to brain Mn accumulation and a parkinsonian-like disorder known as manganism or Mn poisoning. The most common cause of exposure to excess Mn is occupational, and has been documented in miners (5), welders (6), ferroalloy workers (7), battery manufacturers (8), and glass workers (9). Brain Mn accumulation has also been reported in patients receiving total parenteral nutrition therapy (10, 11), patients with hepatic encephalopathy (12), and abusers of ephedrone (methcathinone) (13).

Whole-body Mn homeostasis is maintained by regulating intestinal absorption and excretion of the metal (14). Mn is excreted from the body primarily by hepatobiliary secretion into the gastrointestinal tract for elimination via feces (15). More than a dozen putative Mn transporters (importers and exporters) have been described (16), but few have been rigorously evaluated within the physiological context. Recent genetic studies have revealed a role for solute carrier family 30, member 10 (SLC30A10) in Mn homeostasis, because patients with disruptive *SLC30A10*

Significance

Manganese (Mn) is an essential nutrient that is toxic in excess. Exposure to excess Mn can result in Mn accumulation in the brain and neurological and motor disturbances resembling Parkinson disease. Here, we demonstrate that the transmembrane metal-ion transporter solute carrier family 39, member 14 (SLC39A14) is essential for Mn homeostasis. We provide evidence that SLC39A14 is required for efficient Mn uptake by the liver and pancreas, two organs that are known to actively participate in Mn excretion from the body. Accordingly, loss of SLC39A14 impairs Mn excretion, leading to Mn accumulation in the brain and most other extrahepatic tissues. *Slc39a14*-deficient mice, similar to *SLC39A14*-deficient human patients, display motor deficits, and thus offer a convenient model to study Mn/SLC39A14-related neurotoxicity.

Author contributions: S.J., C.J., B.G., and M.D.K. designed research; S.J., A.A., E.P., R.W., G.G., J.S., A.G., C.J., B.G., and M.D.K. performed research; R.W., S.H., and T.F. contributed new reagents/analytic tools; S.J., A.A., C.J., and M.D.K. analyzed data; and S.J., T.F., C.J., B.G., and M.D.K. wrote the paper.

The authors declare no conflict of interest.

This article is a PNAS Direct Submission. V.C.C. is a guest editor invited by the Editorial Board.

[1]To whom correspondence should be addressed. Email: mknutson@ufl.edu.

This article contains supporting information online at www.pnas.org/lookup/suppl/doi:10.1073/pnas.1720739115/-/DCSupplemental.

mutations display hypermanganesemia, Mn accumulation in the liver and brain, and parkinsonism (17–19). *Slc30a10*-deficient mice also hyperaccumulate Mn in the blood, liver, and brain (20), thus confirming that SLC30A10 participates in Mn homeostasis. Studies in *Caenorhabditis elegans* and various cell lines demonstrate that SLC30A10 is a cell-surface Mn efflux transporter (21–23) and that disease-causing mutations block its trafficking and efflux activity (23, 24). The localization of SLC30A10 to the bile duct epithelium in human liver (19) and to the apical domain of polarized HepG2 cells (25) suggests that SLC30A10 is required for Mn export into bile. As for cellular Mn uptake, the plasma membrane protein divalent metal-ion transporter-1 (DMT1) is frequently cited as the primary Mn^{2+} importer (26–28). Although DMT1 can certainly transport Mn (29), a study of intestine-specific DMT1-null mice demonstrated that it is dispensable for Mn absorption (30). Likewise, Belgrade rats, which are deficient in DMT1, display enhanced uptake of radioactive Mn from the serum into the liver (31), suggesting that DMT1 is dispensable for hepatic Mn homeostasis. On the other hand, SLC39A8, a member of the SLC39A family of metal-ion transporters, is essential for hepatic and whole-body Mn homeostasis, as documented by a recent study of hepatocyte-specific *Slc39a8*$^{-/-}$ mice (32). SLC39A8 localizes to the apical membrane of hepatocytes, where it likely functions to reclaim Mn from the bile.

Recent data indicate that SLC39A14, a close homolog of SLC39A8, is also involved in Mn homeostasis. Although SLC39A14 was first characterized as a zinc transporter (33), we showed that SLC39A14 could also mediate the cellular uptake of iron, Mn, and cadmium (34, 35). Here, using *Slc39a14*$^{-/-}$ mice, we demonstrate that the loss of SLC39A14 results in markedly elevated Mn concentrations in the blood, bone, heart, kidney, and brain, and is associated with motor deficits. While these studies were in progress, Tuschl et al. (36) reported similar findings in human patients carrying loss-of-function mutations in *SLC39A14*. Specifically, patients with homozygous mutations in *SLC39A14* develop juvenile-onset dystonia-parkinsonism associated with elevated Mn concentrations in blood and Mn accumulation in the brain, particularly in the globus pallidus (as assessed by MRI). However, unlike patients with mutations in *SLC30A10*, individuals with *SLC39A14* mutations do not appear to accumulate Mn in the liver (as assessed by liver MRI of one patient). In an effort to elucidate the mechanism underlying the altered Mn homeostasis associated with SLC39A14 deficiency, Tuschl et al. (36) used CRISPR-Cas9 editing to generate zebrafish lacking *slc39a14*. They found that, similar to human patients, *slc39a14*-null zebrafish accumulated Mn in the brain, but not in abdominal viscera (liver, intestine, pancreas, and spleen combined).

The aim of the present study was to utilize *Slc39a14*$^{-/-}$ mice to define the molecular and physiological defects that contribute to the dramatically altered Mn homeostasis resulting from loss of SLC39A14. We also used the *Slc39a14*$^{-/-}$ mice to determine whether reversal of brain Mn accumulation could rescue their motor deficits. Such a question is relevant to human patients with *SLC39A14* mutations, as Mn depletion via chelation is the current treatment strategy in affected individuals (36).

Results

***Slc39a14*$^{-/-}$ Mice Accumulate Mn in Extrahepatic Tissues.** Inductively coupled plasma mass spectroscopy (ICP-MS) was used to measure the concentrations of Mn in a variety of tissues [liver, bone (femur), brain, kidney, pancreas, heart, and spleen] from *Slc39a14*$^{-/-}$ mice and wild-type (WT) littermate controls. Tissues were from mice at 4 and 16 wk of age on a mixed C57BL/6 × 129 genetic background (designated B6;129), similar to the mice we used in a previous study (37). Mn concentrations in the livers of *Slc39a14*$^{-/-}$ mice were found to be 61% lower than in controls at 4 wk of age (Fig. 1*A*) and 35% lower at 16 wk of age (Fig. 1*B*). By contrast, Mn concentrations were elevated in all other tissues of *Slc39a14*$^{-/-}$ mice, except for pancreas, at 4 wk of age (Fig. 1 *A* and *B*). Concentrations of Mn in the brain were 10- and sixfold higher in *Slc39a14*$^{-/-}$ mice than in controls at 4 and 16 wk of age, respectively. Bone was most affected, having Mn concentrations that were 33- and 40-fold higher than controls at 4 and 16 wk of age, respectively (Fig. 1 *A* and *B*).

Livers of *Slc39a14*$^{-/-}$ mice also showed lower concentrations of iron (37% lower at 4 wk), zinc (11% and 15% lower at 4 and 16 wk, respectively), and cobalt (32% and 22% lower at 4 and 16 wk, respectively) (Fig. S1). However, unlike Mn, concentrations of iron, zinc, and cobalt were not elevated in extrahepatic tissues, except for a 15% elevation in femur zinc concentrations at 16 wk of age. Tissue copper concentrations did not differ between *Slc39a14*$^{-/-}$ mice and controls (Fig. S1).

To determine whether the alterations in tissue Mn concentrations in *Slc39a14*$^{-/-}$ mice were replicable and not confounded by their original B6;129 hybrid genetic background, we backcrossed these mice onto the 129S6/SvEvTac strain (designated 129S6) for nine generations. Similar alterations in tissue Mn concentrations were observed in the incipient congenic 129S6 strain at 4 and 52 wk of age (Fig. 1 *C* and *D*). These findings confirm that loss of *Slc39a14* results in an increase in Mn concentrations in most extrahepatic tissues, thus ensuring replicability of the results in mouse models irrespective of their genetic background. Mn concentrations in whole blood, a commonly used indicator of Mn status (38), were also found to be markedly elevated in *Slc39a14*$^{-/-}$ mice (Fig. 1 *C* and *D*). Mn concentrations in the liver, brain, and bone in hemizygous *Slc39a14*$^{+/-}$ mice at 4 and 52 wk of age did not differ from those of WT littermate controls (Fig. S2).

***Slc39a14*$^{-/-}$ Mice Display Impaired Hepatic Uptake of ^{54}Mn.** The lower hepatic Mn concentrations coupled with elevated Mn levels in other tissues (Fig. 1) suggested that *Slc39a14*$^{-/-}$ mice have a liver-specific defect in Mn uptake. To test this hypothesis, we measured the tissue distribution of ^{54}Mn 2 h after i.v. administration of $^{54}MnCl_2$. We observed that the livers of *Slc39a14*$^{-/-}$ mice accumulated 63% less ^{54}Mn than did livers from WT mice (Fig. 2*A*). We additionally found that pancreata

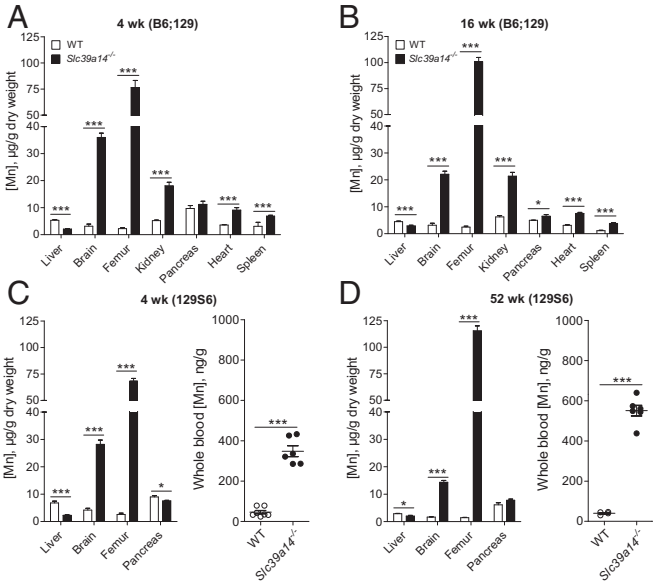

Fig. 1. *Slc39a14*$^{-/-}$ mice exhibit hepatic Mn deficiency and Mn accumulation in other tissues. Mn concentrations in various tissues of *Slc39a14*$^{-/-}$ mice and WT littermate controls were determined by using ICP-MS. (*A* and *B*) Tissues from mixed-background B6;129 male and female mice at 4 and 16 wk of age (n = 5–8 per genotype). (*C* and *D*) Liver, brain, femur (n = 4–5 per genotype). and whole blood (n = 4–7 per genotype) from congenic 129S6 male and female mice at 4 and 52 wk of age. Data represent mean ± SEM. *P < 0.05; ***P < 0.001.

of *Slc39a14*$^{-/-}$ mice accumulated 81% less ^{54}Mn compared with those of WT mice. All other analyzed tissues of *Slc39a14*$^{-/-}$ mice, however, accumulated more ^{54}Mn compared with tissues from WT control littermates. In control animals, most ^{54}Mn was recovered in the liver > kidney > pancreas > other tissues, similar to a previous study of i.v.-administered ^{54}Mn (39).

Given that mice under normal conditions acquire their Mn primarily through the diet, we examined the tissue distribution of ^{54}Mn administered orally via orogastric gavage. Four hours after gavage, 79% of whole-body counts per minute was found in the livers of WT mice (Fig. 2*B*). By contrast, only 7.5% of whole-body counts per minute was found in the livers of *Slc39a14*$^{-/-}$ mice, indicating a dramatic impairment in hepatic uptake/retention of absorbed ^{54}Mn. Accumulation of ^{54}Mn in the pancreas, however, did not differ between WT and *Slc39a14*$^{-/-}$ mice. In all other tissues examined, ^{54}Mn accumulation was markedly higher in *Slc39a14*$^{-/-}$ mice compared with WT control littermates. Overall, *Slc39a14*$^{-/-}$ mice absorbed and retained 7.5-fold more ^{54}Mn than did WT mice (4.1% vs. 0.48% of gavage dose) (Fig. 2*B*). When the relative accumulation of ^{54}Mn in tissues is expressed per gram of fresh weight (40), liver tissue shows the most avid accumulation of ^{54}Mn in WT mice, indicating efficient mechanisms for the uptake/retention of Mn in this organ (Fig. 2*C*). In *Slc39a14*$^{-/-}$ mice, however, the most avid uptake/retention of ^{54}Mn was found in the kidney, femur, and heart tissue.

SLC39A14 Knockdown Impairs Uptake of ^{54}Mn by HepG2 Cells. Mn taken up by the liver accumulates in hepatocytes and is subsequently secreted into the bile (41). To test the hypothesis that SLC39A14 mediates Mn uptake by hepatocytes, we measured ^{54}Mn accumulation in HepG2 cells after suppressing SLC39A14 expression. HepG2 cells, a human hepatoma cell line, were used because they have been shown to take up and release Mn similar to isolated rat hepatocytes (42). We found that siRNA-mediated knockdown of SLC39A14 reduced cellular ^{54}Mn accumulation by 76% when HepG2 cells were incubated with ^{54}Mn for 1 h (Fig. S3). This difference likely reflects a decrease in ^{54}Mn uptake because more than 2 h is required for HepG2 cells to release newly acquired ^{54}Mn (42).

Levels of DMT1 and SLC39A8 in Livers of *Slc39a14*$^{-/-}$ Mice. To determine whether hepatic Mn deficiency in livers of *Slc39a14*$^{-/-}$ mice is associated with compensatory changes in the levels of other known Mn importers, we measured levels of DMT1 and SLC39A8. In livers of mice at 16 wk of age, we found no differences in the levels of DMT1 and SLC39A8 (Fig. S4 *A* and *B*). We also measured levels of transferrin receptor 1 (TfR1), because most Mn in blood plasma is bound to transferrin (43), which can be internalized by binding to TfR1 at the cell surface. Hepatic TfR1 levels did not differ between WT and *Slc39a14*$^{-/-}$ mice (Fig. S4*C*). In livers of mice at 4 wk of age, we found that levels of DMT1 and TfR1 were elevated in *Slc39a14*$^{-/-}$ mice (Fig. S5 *A* and *C*). However, at this age, not only were hepatic Mn levels lower in the KO mice, but hepatic Fe levels were also lower in the KO mouse (Fig. S1). Thus, it seems likely that DMT1 and TfR1 levels are responding not to Mn deficiency per se, but rather to iron deficiency, as seen in previous studies of iron-deficient liver (44). Importantly, despite the up-regulation of DMT1 and TfR1, hepatic Mn levels were still 61% lower in *Slc39a14*$^{-/-}$ mice compared with WT controls (Fig. 1*A*), indicating that up-regulation of DMT1 and TFR1 cannot compensate for loss of SLC39A14.

***Slc39a14*$^{-/-}$ Mice Display Impaired ^{54}Mn Excretion.** Mn is excreted nearly exclusively (99%) via the gastrointestinal tract, mainly from bile, but also by pancreatic and intestinal secretions (15, 45). To assess Mn excretion, *Slc39a14*$^{-/-}$ mice and their WT littermates were given i.v. ^{54}Mn and then housed individually in metabolic cages for 6 h to allow for collection of feces. The 6-h time point was selected based on a previous study in mice showing that Mn is maximally excreted in the feces 4–6 h after i.v. administration (39). At the time of euthanasia, major tissues were harvested as before, but this time, gallbladder [indicative of biliary excretion (46)], intestinal tract (from the proximal small intestine to the anus), and gut luminal contents were also

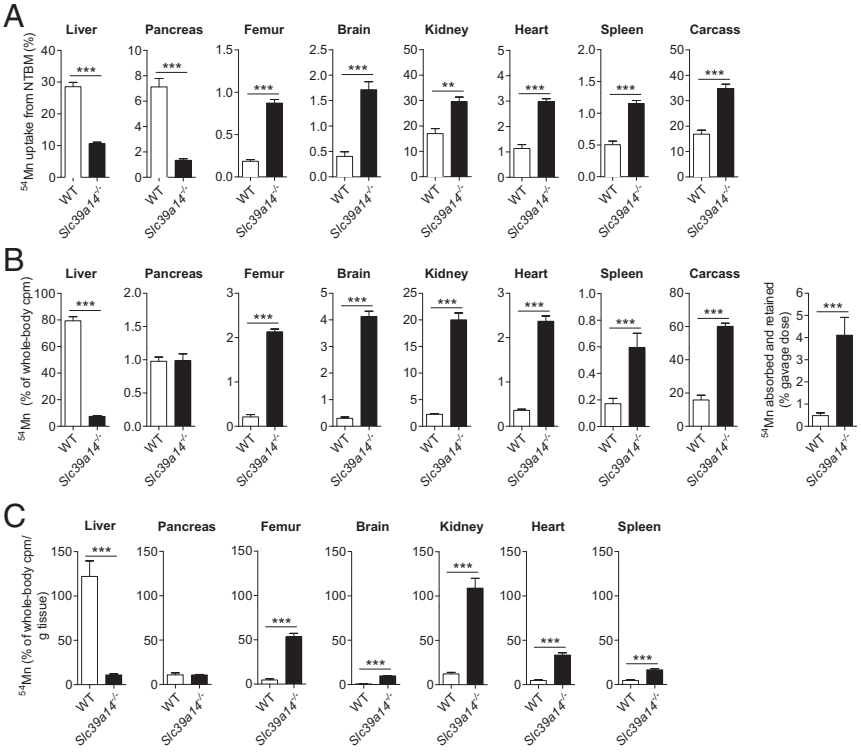

Fig. 2. Tissue distribution of i.v. or orally administered ^{54}Mn. (*A*) WT and *Slc39a14*$^{-/-}$ mice at 20 wk of age were injected via tail vein with 2 μCi [^{54}Mn]$MnCl_2$. Two hours later, mice were killed and whole-body and tissue counts per minute (cpm) were determined by γ-counting [WT: $n = 4$, $n = 1$ male (M), $n = 3$ female (F); *Slc39a14*$^{-/-}$: $n = 5$, $n = 3$ M, $n = 2$ F]. (*B*) WT and *Slc39a14*$^{-/-}$ mice at 4–5 wk of age were administered 2 μCi [^{54}Mn]$MnCl_2$ via orogastric gavage. Four hours later, mice were killed and whole-body and tissue cpm were determined by γ-counting [WT: $n = 4$, $n = 2$ M, $n = 2$ F; *Slc39a14*$^{-/-}$: $n = 4$, $n = 2$ M, $n = 2$ F]. (*C*) Data in *B* normalized per gram of tissue. Data represent mean ± SEM. $^{**}P < 0.01$; $^{***}P < 0.001$.

collected. Compared with WT mice, *Slc39a14*$^{-/-}$ mice had 85% less ^{54}Mn in the gallbladder, 60% less ^{54}Mn in gut luminal contents, and 50% less ^{54}Mn in feces, consistent with diminished excretion of Mn into the gastrointestinal tract (Fig. 3*A*). At this 6-h time point, the distributions of ^{54}Mn in the liver, pancreas, femur, brain, kidney, heart, spleen, and carcass of WT and *Slc39a14*$^{-/-}$ mice (Fig. 3*A*, *Lower*) were similar to those observed 2 h after i.v. administration of ^{54}Mn (Fig. 2*A*). Thus, the diminished ^{54}Mn excretion by *Slc39a14*$^{-/-}$ mice 6 h after i.v. administration of Mn appears to be due to impaired uptake of plasma ^{54}Mn by the liver and pancreas.

Fecal excretion of i.v.-administered ^{54}Mn was further assessed at 24 and 48 h, which additionally allowed for the collection and measurement of ^{54}Mn in the urine (Fig. 3*B*). Fecal excretion of ^{54}Mn by *Slc39a14*$^{-/-}$ mice was 35% and 31% lower at 24 and 48 h, respectively, compared with WT controls. By contrast, urinary ^{54}Mn excretion was two- to threefold higher in *Slc39a14*$^{-/-}$ mice compared with WT mice. It should be noted, however, that less than 1% of the i.v. dose of ^{54}Mn was recovered in the urine, consistent with previous studies in mice (39).

***Slc39a14*$^{-/-}$ Mice Accumulate Mn in Specific Brain Regions.** To determine where Mn accumulates in the brain of *Slc39a14*$^{-/-}$ mice, we used laser ablation (LA)-ICP-MS, a recently developed method that can quantify and image metal distributions in mouse brain sections (47). Distributions of Mn in the *Slc39a14*$^{-/-}$ mouse brain are shown at three different maximum detection thresholds (10, 7, and 5 μg/g) (Fig. 4 *A*, *C*, and *E*). The highest concentrations of Mn (at least 10 μg/g) were found in the nucleus of the lateral lemniscus and parts of the cerebellum (Fig. 4*A*). Parts of the globus pallidus, the dorsal nucleus raphe, and the pons had Mn concentrations of at least 7 μg/g (Fig. 4*C*), and the vestibular nucleus and the zona incerta had Mn concentrations of at least 5 μg/g (Fig. 4*E*). Distributions of Mn at different thresholds are also shown for WT mouse brain, but the thresholds are 10-fold lower to account for the lower brain Mn concentrations in WT mice (Fig. 4 *B*, *D*, and *F*). In general, the regions with the highest Mn concentrations in WT mouse brain were the same regions as in the *Slc39a14*$^{-/-}$ mouse brain. Thus, while loss of SLC39A14 clearly affects the magnitude of Mn accumulation in the brain, it does not seem to affect its regional distribution (Fig. 4). Loss of SLC39A14 also does not affect the regional distribution of iron, zinc, or copper (Fig. S6).

Dietary Mn Alters Tissue Mn Concentrations in *Slc39a14*$^{-/-}$ Mice. Our data show that Mn concentrations in the *Slc39a14*$^{-/-}$ mouse brain are elevated (~10-fold normal) as early as 3 wk of age (Fig. S6). Given that this Mn accumulated before weaning, we hypothesized that brain Mn accumulation could be diminished/reversed by feeding weanling *Slc39a14*$^{-/-}$ mice a low-Mn diet. Conversely, given the impairment in Mn excretion in *Slc39a14*$^{-/-}$ mice, we hypothesized that brain Mn levels would increase markedly if the mice were fed a high-Mn diet. We therefore conducted a 30-d feeding study in which weanling WT and *Slc39a14*$^{-/-}$ mice were fed purified AIN-93G diets that contained either low, normal, or high concentrations of Mn (0, 10, and 2,400 ppm Mn, respectively). The high-Mn diet was based on a previous study that found no toxic symptoms when mice were fed diets containing up to 2,400 ppm Mn (48). Over the 30-d feeding period, body weights did not differ among WT mice fed the different diets (Fig. 5*A*). The *Slc39a14*$^{-/-}$ animals fed the 0- and 10-ppm diets tended to weigh less than the WT mice throughout the study, but growth rates were similar to those of WT mice. *Slc39a14*$^{-/-}$ animals fed the 2,400-ppm diet, however, rapidly lost weight and had to be killed on day 7 of the feeding study. In *Slc39a14*$^{-/-}$ mice fed the low-Mn diet for 30 d, brain Mn concentrations did not differ ($P = 0.079$) from those of WT mice fed a low-Mn diet (Fig. 5*B*), indicating that a low-Mn diet is able to reverse brain Mn accumulation in *Slc39a14*$^{-/-}$ mice. The high-Mn diet, when fed for only 7 d to *Slc39a14*$^{-/-}$ mice, resulted in an accumulation of brain Mn to levels over 50-fold normal. Bone Mn concentrations were also elevated in these animals (nearly 1,200-fold normal). Interestingly, a low-Mn diet was

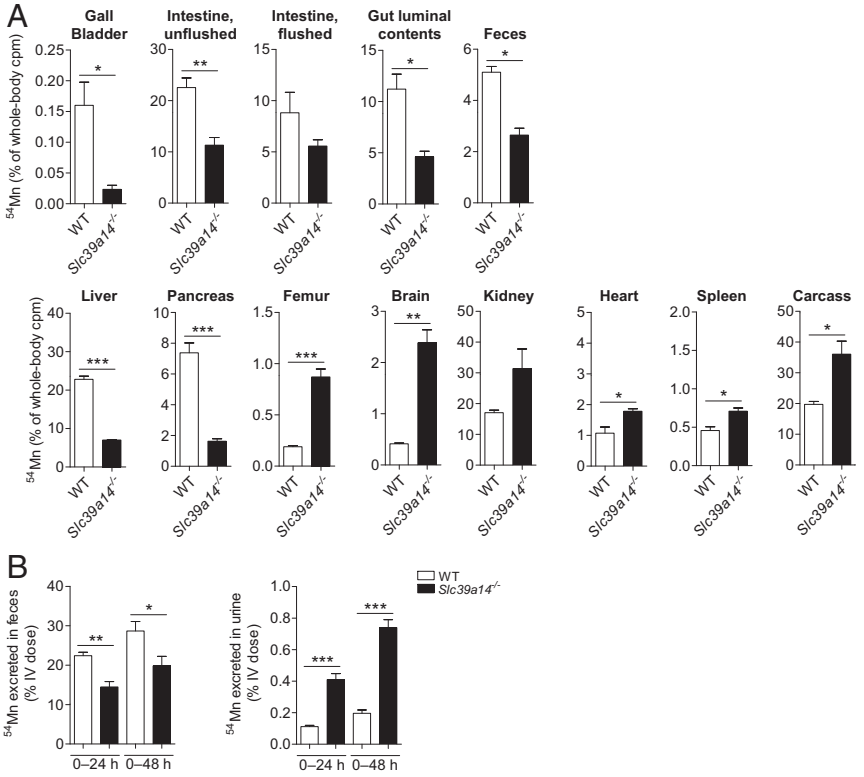

Fig. 3. Loss of SLC39A14 impairs Mn excretion. (*A*) WT and *Slc39a14*$^{-/-}$ mice at 20–32 wk of age were injected via tail vein with 2 μCi [^{54}Mn]$MnCl_2$ and housed individually in metabolic cages. Six hours later, mice were killed and whole-body, tissue, gut luminal contents, and fecal counts per minute (cpm) were determined by γ-counting [WT: $n = 3$, $n = 1$ male (M), $n = 2$ female (F); *Slc39a14*$^{-/-}$: $n = 3$, $n = 1$ M, $n = 2$ F]. (*B*) WT and *Slc39a14*$^{-/-}$ mice at 8–12 wk of age were injected via tail vein with 2 μCi [^{54}Mn]$MnCl_2$ and housed individually in metabolic cages. Feces and urine were collected at 24 and 48 h, and cpm was determined by γ-counting (WT: $n = 5$ M; *Slc39a14*$^{-/-}$: $n = 3$ M). Data represent mean ± SEM. *$P < 0.05$; **$P < 0.01$; ***$P < 0.001$.

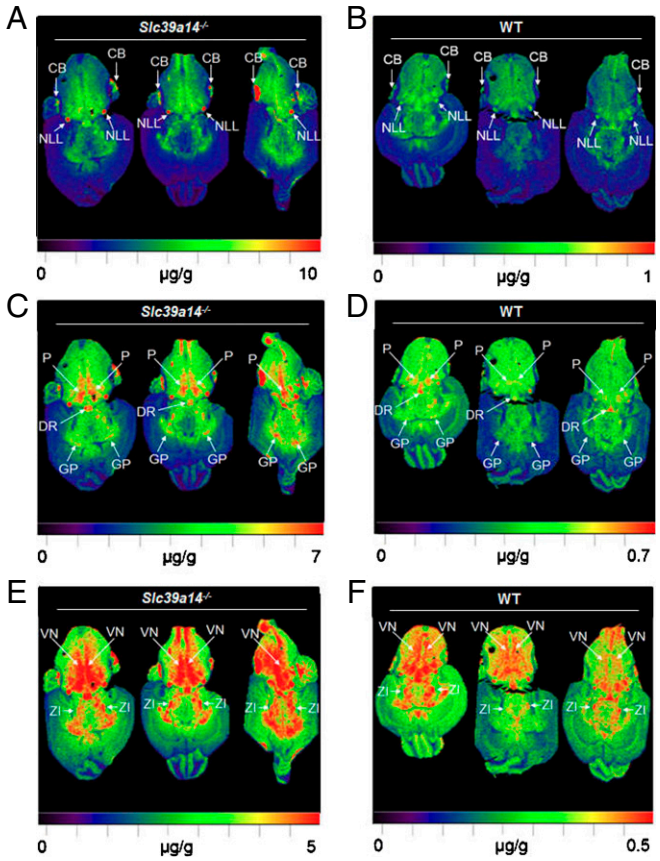

Fig. 4. Regional distribution and accumulation of Mn in *Slc39a14*$^{-/-}$ mouse brain. LA-ICP-MS images of *Slc39a14*$^{-/-}$ mouse brain [$n = 3$, $n = 1$ male (M), $n = 2$ female (F)] shown at three different maximum thresholds: 10, 7, and 5 μg/g (*A*, *C*, and *E*) compared with WT mouse brain ($n = 3$, $n = 1$ M, $n = 2$ F) shown at lower thresholds: 1, 0.7, and 0.5 μg/g (*B*, *D*, and *F*). CB, cerebellum; DR, dorsal nucleus raphe; GP, globus pallidus; NLL, nucleus of the lateral lemniscus; P, pons; VN, vestibular nucleus; ZI, zona incerta.

not able to efficiently reverse Mn accumulation in the bone of *Slc39a14*$^{-/-}$ mice. In WT mice fed the high-Mn diet for 30 d, the liver accumulated the highest concentration of Mn, followed by the bone and then the brain (Fig. 5*B*). The higher liver Mn concentrations in WT animals fed the high-Mn diet for only 7 d compared with 30 d may relate to age differences, as younger animals have been shown to absorb and retain more Mn than older animals (49). After only 7 d of feeding the high-Mn diet, *Slc39a14*$^{-/-}$ mice accumulated 64% less Mn in the liver than did WT mice. When hemizygous (*Slc39a14*$^{+/-}$) mice were fed the high-Mn diet for only 7 d, they accumulated twice as much Mn in the brain and eightfold as much Mn in the bone as did WT mice. Concentrations of iron, zinc, and copper in the brain, bone, and liver of WT, *Slc39a14*$^{-/-}$, and *Slc39a14*$^{+/-}$ mice from this feeding study are shown in Fig. S7.

***Slc39a14*$^{-/-}$ Mice Display Motor Impairments That Are Not Corrected by a Low-Mn Diet.** In initial studies of motor function, we compared WT and *Slc39a14*$^{-/-}$ mice ($n = 2$–3 per sex per genotype) on the B6;129 background at 12 and 52 wk of age and on the 129S6 background at 52 wk of age (Fig. S8). We also compared WT and hemizygous *Slc39a14*$^{+/-}$ mice ($n = 2$–4 per sex per genotype) on the B6;129 background at 12 and 52 wk of age (Fig. S9). Behavioral analyses utilizing the pole test, beam-crossing test, and rotarod test suggested motor deficits in *Slc39a14*$^{-/-}$ mice (Fig. S8), but not in *Slc39a14*$^{+/-}$ animals (Fig. S9). On these genetic backgrounds, *Slc39a14*$^{-/-}$ mice generally weighed less than WT mice, whereas *Slc39a14*$^{+/-}$ mice did not (Fig. S10). Given that sex-specific differences have been reported in mouse behavioral tests, including the rotarod test (50, 51), we repeated the behavioral tests using larger sample sizes of both male and female mice ($n = 8$–9 per sex per genotype). Moreover, to determine whether reversal of brain Mn accumulation could rescue the motor deficits in *Slc39a14*$^{-/-}$ mice, we evaluated in parallel similar numbers of male and female mice that were fed a purified low-Mn diet (0.5 ppm Mn) from weaning to ∼15 wk of age. In this feeding study, the control purified diet was formulated to contain 100 ppm Mn to approximate the level of Mn in standard chow used in the initial behavioral tests. For consistency between low-Mn diet feeding studies, mice in the second feeding study were on the same background as those used in the first study (i.e., 129 + Ter/SvJcl × C57BL/6 × Balb/cJ). Mice were weighed at 10.7 wk of age (before the first test) using the SHIRPA (SmithKline Beecham Pharmaceuticals; Harwell, Medical Research Council Mouse Genome Centre and Mammalian Genetics Unit; Imperial College School of Medicine at St Mary's; Royal London Hospital, St. Bartholomew's and the Royal London School of Medicine Phenotype Assessment) screen and at 14.6 wk of age [before the last test (rotarod test)]. All mice increased their weight during that period [$F(1,56) = 155.8$, $P < 0.001$], with no significant differences between genotype and treatment. Body weights at 14.6 wk of age are shown in Fig. 6*A*. Females were significantly lighter than males [21.3 ± 0.4 g and 26.2 ± 0.4 g for females and males, respectively; $F(1,56) = 84.7$, $P < 0.001$]. Females also gained less weight than did males [$F(1,56) = 7.7$, $P < 0.01$, age by sex interaction effect]. None of the other interactions were significant at $\alpha = 0.05$.

Physical condition and reflexes. Most of the *Slc39a14*$^{-/-}$ mice developed torticollis, which occurred independent of the experimental diet (16 of 17 mice maintained on the control diet and 12 of 17 *Slc39a14*$^{-/-}$ mice maintained on the low-Mn diet showed visible torticollis; $Z = -1.8$, $P = 0.08$, Mann–Whitney *U* test). The *Slc39a14*$^{-/-}$ mice did not differ from their control WT littermates in respiration and tremor levels, transfer arousal, palpebral closure, piloerection, pinna reflex, limb grasping, wire maneuver, or negative geotaxis (SHIRPA screen) irrespective of their genotype and dietary treatment. However, the qualitative observations revealed that the *Slc39a14*$^{-/-}$ mice were less active in a new large cage, and they had difficulties in rearing, often falling back while attempting to rear. The most striking difference was in the righting reflex. Whereas all WT mice showed a righting reflex, *Slc39a14*$^{-/-}$ mice mostly failed in this task. The inability to right themselves was observed in 15 of 17 *Slc39a14*$^{-/-}$ mice in each diet treatment group.

Motor behavior: Pole-descent test. The *Slc39a14*$^{-/-}$ mice showed longer latencies of descending the pole than did the WT mice [$F(1,56) = 10.4$, $P < 0.01$; Fig. 6*B*]. Also, males showed longer descent times than females [$F(1,56) = 6.2$, $P < 0.05$; Fig. 6*B*]. The treatment (diet group) and the interactions between the factors were not significant at $\alpha = 0.05$. The times it took the mice to orient themselves head-down were not significant between the experimental factors.

Beam-traversing test. The time to traverse either the wide or narrow beam (Fig. 6 *C* and *D*, respectively) was similar between the *Slc39a14*$^{-/-}$ mice and their WT counterparts. Overall, females traversed the beams faster than males [26.2 ± 5.5 and 47.4 ± 5.5 s for females and males, respectively; $F(1,56) = 7.5$, $P < 0.01$]. Also, the mice took longer to traverse the wide beam than the narrow beam [$F(1,56) = 14.4$, $P < 0.001$]. Although counterintuitive, the mice were likely still learning the task at that stage, despite the fact that they were habituated to the test 1 d before the test. None of the other factors and interactions were significant. There were no differences in the number of pauses, slips, and falls off the beam between the two diets. *Slc39a14*$^{-/-}$ mice, however, slipped more often on the wide and narrow beams than did the WT controls ($Z = -4.5$, $P < 0.001$ and $Z = -6.4$, $P < 0.001$ for wide beam and narrow beam, respectively, Wilcoxon two-tail test). Also, the *Slc39a14*$^{-/-}$ mice fell more often from

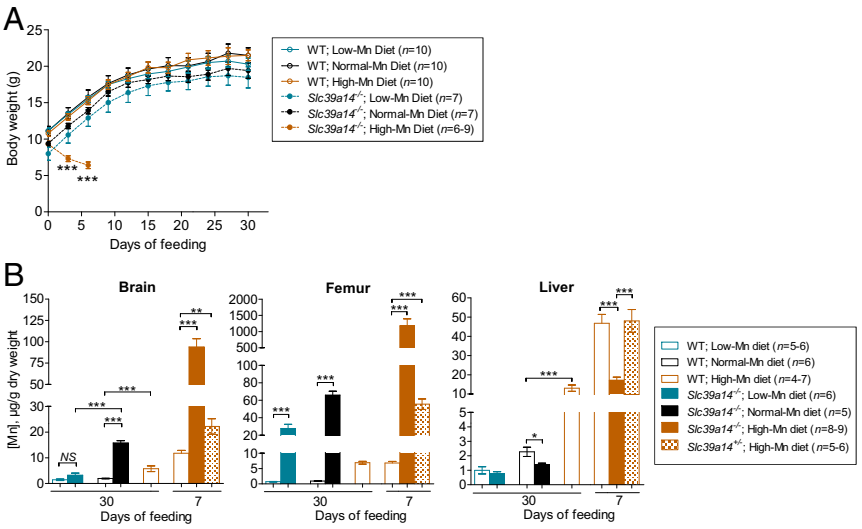

Fig. 5. Effect of dietary Mn concentration on growth and tissue Mn concentrations in *Slc39a14*$^{-/-}$ mice. (*A*) Growth curves of weanling mice fed a low-Mn diet [WT: $n = 10$, $n = 5$ male (M), $n = 5$ female (F); *Slc39a14*$^{-/-}$: $n = 7$, $n = 3$ M, $n = 4$ F], normal-Mn diet (WT: $n = 10$, $n = 5$ M, $n = 5$ F; *Slc39a14*$^{-/-}$: $n = 7$, $n = 2$ M, $n = 5$ F), or high-Mn diet (WT: $n = 10$, $n = 5$ M, $n = 5$ F) for 30 d (or only 7 d for *Slc39a14*$^{-/-}$ mice fed the high-Mn diet; $n = 6$–9, $n = 4$–6 M, $n = 2$–3 F). Data represent mean ± SD. ***$P < 0.001$. (*B*) Mn concentrations in the brain, femur, and liver of mice fed the low-Mn diet (WT: $n = 5$–6, $n = 3$, $n = 2$–3 F; *Slc39a14*$^{-/-}$: $n = 6$, $n = 3$ M, $n = 3$ F), normal-Mn diet (WT: $n = 6$, $n = 3$ M, $n = 3$ F; *Slc39a14*$^{-/-}$: $n = 5$, $n = 2$ M, $n = 3$ F), or high-Mn diet (WT: $n = 4$–5, $n = 2$ M, $n = 2$–3 F) for 30 d [or only 7 d for *Slc39a14*$^{-/-}$ mice fed the high-Mn diet ($n = 8$–9, $n = 6$ M, $n = 2$–3 F)]. For comparison, tissues from WT ($n = 6$–7, $n = 2$–3 M, $n = 3$–5 F) and hemizygous *Slc39a14*$^{+/-}$ mice ($n = 5$–6, $n = 2$–3 M, $n = 3$ F) were also analyzed after only 7 d of feeding. Data represent mean ± SEM. *$P < 0.05$; **$P < 0.01$; ***$P < 0.001$. *NS*, nonsignificant.

the beams (three mice from the wide beam and 10 mice from the narrow beam) than did the WT mice ($Z = -3.0$, $P < 0.001$), which did not fall at all during the test. The mice of both genotypes showed similar numbers of pauses on both beams, which likely contributed to comparable traversing times of each beam (Fig. 6 *C* and *D*).

Rotarod test. When challenged in the rotarod test, the *Slc39a14*$^{-/-}$ mice stayed on the rotating rod for significantly shorter times than did their WT littermates, after controlling for the body weight of mice [$F(1,56) = 55.2$, $P < 0.001$; Fig. 6 *E* and *F*]. Although performance in the test was similar between sexes, the WT females stayed longer on the rod, whereas the *Slc39a14*$^{-/-}$ females stayed shorter on the rod than their respective male counterparts [$F(1,55) = 5.3$, $P < 0.05$, genotype by sex interaction effect]. The WT mice showed improvement and stayed longer on the accelerated rod as training progressed (sessions 2 and 3), irrespective of the type of diet, in contrast to *Slc39a14*$^{-/-}$ mice, which performed comparably across sessions [$F(2,110) = 3.24$, $P < 0.05$, genotype by session by treatment (diet) interaction effect]. None of the other main factors, including treatment; sex; session; and other second-, third-, and fourth-order interactions, were significant at $\alpha = 0.05$. The speed of the rotating rod (revolutions per minute) was highly correlated with the latencies to fall ($0.98 < P < 1.0$ in all tests), and is therefore not reported. Mice were killed 2 d after the last behavioral test (at ∼15 wk of age), and tissues were harvested. Randomly selected brain samples (three males and three females from each treatment group, $n = 24$ total) were analyzed by ICP-MS for determination of metal concentrations. Brain Mn concentrations in *Slc39a14*$^{-/-}$ mice fed the control diet were ∼15-fold higher than those of WT controls (Fig. 6*G*). In *Slc39a14*$^{-/-}$ mice fed the low-Mn diet, brain Mn concentrations were almost normal (i.e., only onefold higher than WT controls), whereas concentrations of iron, zinc, and copper were normal (Fig. S11).

Discussion

A main finding from the present study is that Mn concentrations are markedly altered in nearly all tissues of *Slc39a14*$^{-/-}$ mice, and the alterations are independent of age, sex, and genetic background. We therefore conclude that SLC39A14 is essential for Mn homeostasis. Given that SLC39A14 was first identified as a zinc transporter (33), and shortly thereafter as an iron transporter (34), the early studies of *Slc39a14*$^{-/-}$ mice focused on characterizing the zinc and iron status of these animals. In the original characterization of the mice, Hojyo et al. (52) reported that hepatic zinc concentrations were ∼30% lower in *Slc39a14*$^{-/-}$ mice compared with controls. Other studies, however, reported no alterations in hepatic zinc levels in *Slc39a14*$^{-/-}$ mice under normal conditions (53–55). Here, we find that hepatic zinc concentrations are 11–15% lower in *Slc39a14*$^{-/-}$ mice at 4–16 wk of age, but were not significantly different from controls at 52 wk of age [95.1 ± 2.2 µg/g (WT) vs. 92.2 µg/g (*Slc39a14*$^{-/-}$), $n = 4$–5 per group]. With respect to iron status, we find that hepatic iron concentrations in *Slc39a14*$^{-/-}$ mice are ∼35% lower at 4 wk of age, but not at older ages, similar to our previous study (37). By contrast, other studies have reported no decreases in hepatic iron concentrations in *Slc39a14*$^{-/-}$ mice (52, 54). Apparent inconsistencies among these studies likely relate to differences in mouse age, sex, genetic background, and perhaps diet. In the present study, expansion of the analysis of zinc and iron to six other tissues (bone, brain, kidney, pancreas, heart, and spleen) revealed that loss of *Slc39a14* does not affect zinc and iron concentrations in the brain, kidney, pancreas, and heart, but is associated with modest changes in bone zinc concentrations and splenic iron concentrations (but only at 16 wk of age). Overall, the relatively minor perturbations in the homeostasis of zinc or iron contrast markedly to the major alterations in Mn homeostasis in *Slc39a14*$^{-/-}$ mice, suggesting that Mn is a main physiological substrate of SLC39A14. Indeed, while our manuscript was under revision, three groups independently reported the prominent alterations in Mn metabolism in *Slc39a14*$^{-/-}$ mice (i.e., elevated Mn concentrations in blood and the brain, but not in the liver) (25, 56, 57), thus reaffirming that SLC39A14 is required for normal Mn homeostasis.

Dietary Mn, likely as Mn^{2+}, is absorbed by the intestine and enters portal blood, where it may remain free or become bound to α-2 macroglobulin or albumin (4, 58). Regardless of the form, Mn in portal blood is rapidly taken up by the liver via first-pass extraction (4, 58). Data from the present study suggest that hepatic first-pass clearance of Mn is mediated primarily by SLC39A14, as livers from *Slc39a14*$^{-/-}$ mice accumulated markedly less ^{54}Mn than did livers of WT controls after orogastric gavage of $^{54}MnCl_2$. The diminished hepatic ^{54}Mn accumulation in *Slc39a14*$^{-/-}$ mice does not likely result from impaired intestinal absorption because the mice absorbed and retained sevenfold more ^{54}Mn than did control mice. Indeed, the relative accumulation of orally administered ^{54}Mn among tissues in *Slc39a14*$^{-/-}$ mice was similar to the alterations in tissue Mn concentrations in these animals (i.e., reduced Mn levels in the liver, notably elevated Mn levels in other tissues except for the pancreas). Our experiments with i.v.-administered ^{54}Mn further suggest that SLC39A14 is essential for hepatic (and pancreatic) clearance of Mn in the systemic circulation. With i.v. administration, however, all tissues are similarly exposed to ^{54}Mn, as opposed to oral administration and intestinal absorption, which expose the liver first to the metal. Such a difference in Mn

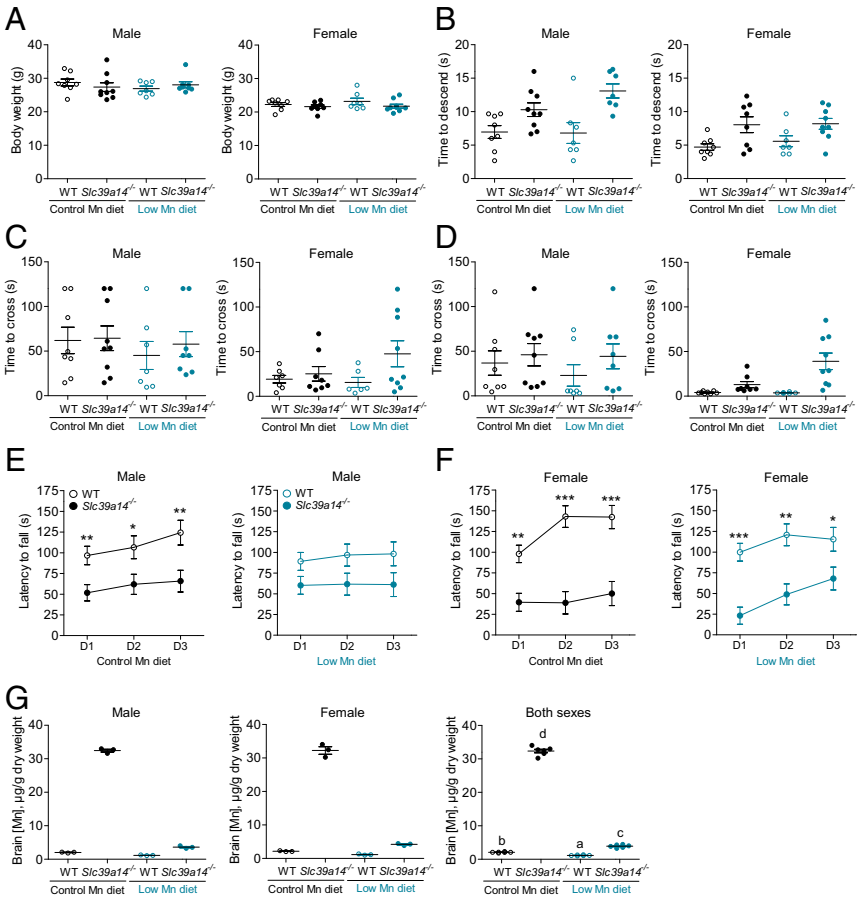

Fig. 6. *Slc39a14*$^{-/-}$ mice display motor impairments that are not corrected by a low-Mn diet. WT and *Slc39a14*$^{-/-}$ mice were maintained on a control-Mn diet (n = 8–9 per genotype per sex) or a low-Mn diet (n = 7–9 per genotype per sex) from weaning. (*A*) Mouse body weights at 14.6 wk of age. Mice were tested in a battery of locomotor tests, including the pole test (*B*), wide (2.5-cm) beam-crossing test (*C*), narrow (1.7-cm) beam-crossing test (*D*), and rotarod test (*E* and *F*). (*G*) Mn concentrations in randomly selected brains from each group (n = 6, n = 3 male, n = 3 female) at ∼15 wk of age. D1, D2, and D3 denote day 1, day 2, and day 3, respectively. Data represent mean ± SEM. *$P < 0.05$; **$P < 0.01$; ***$P < 0.001$. In *G*, means without a common superscript letter differ significantly ($P < 0.05$).

exposure may explain why pancreatic accumulation of ^{54}Mn was diminished in *Slc39a14*$^{-/-}$ mice after i.v. ^{54}Mn but not after orally administered ^{54}Mn. Our studies additionally demonstrate that the bone, brain, kidney, heart, and spleen have SLC39A14-independent Mn uptake mechanisms.

The liver plays an important role in Mn homeostasis by secreting excess Mn into the bile for elimination in feces (15). Accordingly, an impairment in Mn uptake by the liver would be expected to decrease gastrointestinal excretion of the metal, which is what we observed in *Slc39a14*$^{-/-}$ mice. Experiments in rats have shown that bile-duct ligation diminishes, but does not abolish, Mn excretion, thus indicating the existence of alternative routes of Mn excretion (59). Indeed, hepatocyte-specific inactivation of *Slc39a14* in mice does not result in Mn loading in extrahepatic tissues under normal conditions (57). In response to a high-Mn diet, however, hepatocyte-specific *Slc39a14*-null mice do load Mn not only in the brain but also in the pancreas and intestine, consistent with data suggesting that Mn can be excreted via the pancreas and/or intestine when the hepatobiliary route is blocked (59, 60). Our i.v. injection experiments indicate diminished accumulation of ^{54}Mn in the pancreas of *Slc39a14*$^{-/-}$ mice, suggesting that impaired uptake and secretion of ^{54}Mn by the pancreas may contribute to their decreased gastrointestinal excretion of Mn. Whatever the routes of Mn excretion in *Slc39a14*$^{-/-}$ mice, they are insufficient and unable to prevent Mn accumulation in the body. The inability to efficiently excrete excess Mn was clearly evident when the *Slc39a14*$^{-/-}$ mice were fed a high-Mn diet: Brain and femur Mn concentrations increased ∼50- and 1,000-fold normal, respectively.

The elevated blood and brain Mn levels in *Slc39a14*$^{-/-}$ mice are similar to what has been reported for humans with loss-of-function mutations in *SLC39A14* (36). In the human study (36), MRI analysis was performed on one patient's liver, leading the authors of that study to conclude that Mn does not accumulate in the liver in affected individuals. Our results suggest that studies of human patients should include, whenever possible, quantitative measurements of Mn in the liver, bone, and other tissues. MRI analyses of brains of patients with *SLC39A14* mutations (3 and 17 y of age) indicated the most prominent Mn accumulation in the globus pallidus, striatum, pituitary, dorsal pons, and cerebellum (36). Our LA-ICP-MS analysis of brain sections from *Slc39a14*$^{-/-}$ mice also indicated notable Mn accumulation in the globus pallidus, pons, and cerebellum, with the highest Mn concentrations detected in parts of the cerebellum and in the nucleus of the lateral lemniscus. Differences in brain Mn accumulation between humans and rodents have been noted by others (61, 62). Importantly, the regions accumulating the most Mn in the brain of *Slc39a14*$^{-/-}$ mice were the same regions with the highest normal physiological Mn concentrations in the brains of WT mice, suggesting that loss of SLC39A14 does not alter the regional distribution of Mn within the brain. Studies at the cellular level will be needed to define the contribution of SLC39A14 to Mn uptake by different neural cell types.

Environmental exposure to increased levels of Mn, and its resultant deposition in the brain, leads to manganism in humans, which manifests behaviorally as motor dysfunction (63). Moreover, children who carry homozygous loss-of-function mutations in *SLC39A14* showed elevated levels of brain Mn coinciding with progressive dystonia and parkinsonism (36). Consequently, we focused our primary phenotypic evaluation of the *Slc39a14*$^{-/-}$ mouse model on locomotor behavior to establish its external validity to human disease. Two of the recently published papers on *Slc39a14*$^{-/-}$ mice reported motor deficits in these animals, but these studies grouped both male and female mice in the behavioral tests, and some tests had insufficient sample sizes (e.g., n = 3–4) (56, 57). Here, by assessing eight to nine mice of each

sex and genotype, we found significant differences in the performance of male and female mice in the pole test, beam-crossing test, and rotarod test, thus highlighting the importance of sex as a factor in behavioral studies of these mice. The choice of tests and the order of administration followed increasing difficulty of motor tasks, with the pole and beam tests focusing mainly on spontaneous motor behavior (descending a vertical pole and traversing a horizontal beam, respectively). Both tasks require precise body alignment and coordinated movement of limbs, and have been used extensively to identify motor impairments with underlying CNS mechanisms (64–66). Although *Slc39a14*$^{-/-}$ mice had longer descent times than WT mice in the pole test, they did not exhibit longer beam-crossing times. In the beam-crossing tests, however, *Slc39a14*$^{-/-}$ mice frequently slipped on/fell from the beams, indicating deficits in balance and coordination. The rotarod test, which addresses motor balance and coordination in a more rigorous manner (67–69), revealed the most pronounced genotype differences, with *Slc39a14*$^{-/-}$ mice significantly and consistently showing shorter latencies to fall compared with their WT littermates. Although these tests are typically used to evaluate impairments with underlying nervous system mechanisms (70), we cannot exclude the confounding contribution of the peripheral effects of Mn accumulation on the motor impairment observed in *Slc39a14*$^{-/-}$ mice. This issue is particularly important because of the observed high accumulation of Mn in bones in this model. Another potential confounder is torticollis, which was visible in 82% (28 of 34) of the *Slc39a14*$^{-/-}$ mice used in the sex-segregated behavioral testing experiment. Unfortunately, the effect of torticollis on motor function cannot be reliably determined from this experiment because only six of 34 *Slc39a14*$^{-/-}$ mice did not have torticollis. Nonetheless, inspection of their individual behavioral data revealed that mice without torticollis did not generally perform better on any of the tests than did those with torticollis.

In the study of patients with loss-of-function mutations in *SLC39A14*, heterozygous parents were reported to have normal Mn levels (36). Similarly, we found that hemizygous *Slc39a14*$^{+/-}$ mice had normal levels of Mn in various tissues (i.e., liver, brain, bone) and locomotor function similar to their WT littermates. However, when *Slc39a14*$^{+/-}$ mice were fed a high-Mn diet, they accumulated more Mn in the brain and bone than did WT littermate controls. We therefore speculate that asymptomatic heterozygous carriers for disruptive mutations in *SLC39A14* might be more susceptible to Mn toxicity when exposed to high levels of Mn, and this may help to explain why certain individuals rapidly develop symptoms of Mn toxicity, whereas others exposed to the same conditions do not (71).

Treatment of Mn-exposed humans involves cessation of exposure, and in some cases, treatment with i.v. $Na_2CaEDTA$, which chelates Mn in the blood and increases its urinary excretion (72). Tuschl et al. (36) treated two patients with *SLC39A14* mutations with $Na_2CaEDTA$, one starting treatment at 5 y of age and the other at 17 y of age. The younger patient showed dramatic clinical improvement by regaining the ability to walk independently, whereas the older patient continued to deteriorate despite mobilization of Mn stores. Xin et al. (57) reported that 5-mo-old *Slc39a14*$^{-/-}$ mice treated with $Na_2CaEDTA$ for 4 wk performed better on the rotarod than did saline-treated *Slc39a14*$^{-/-}$ controls. The *Slc39a14*$^{-/-}$ mice treated with $Na_2CaEDTA$ also had serum Mn concentrations that were 50% lower than those in saline-treated *Slc39a14*$^{-/-}$ controls, but the levels were still 10-fold normal and brain Mn concentrations are not reported. Here, we found that feeding a low-Mn diet to *Slc39a14*$^{-/-}$ mice from weaning to 12 wk of age lowered brain Mn concentrations about 10-fold to nearly normal levels but did not improve performance in the rotarod test or any other behavioral test. This finding suggests that the motor deficits represent lasting effects of early-life Mn exposure, as brain Mn concentrations are markedly elevated in *Slc39a14*$^{-/-}$ mice as early as 3 wk of age (Fig. S6). Studies in rats have shown that male rat pups exposed to high-dose i.p. Mn during postnatal days 8–12 performed poorly on the rotarod test as adults on postnatal day 65 when brain Mn concentrations had returned to normal (73). Further investigation is required to determine whether prevention/mitigation of Mn exposure to *Slc39a14*$^{-/-}$ mice in utero and before weaning will correct their motor deficits.

An interesting observation from the present study is that Mn accumulated to the greatest extent in the bone of *Slc39a14*$^{-/-}$ mice, suggesting that the skeleton is the main extrahepatic reservoir for excess Mn. Mn accumulation in bone of *Slc39a14*$^{-/-}$ mice most likely results from increased deposition rather than decreased release, because the biological half-life of Mn in bone is relatively long [i.e., 77 d in the rat (3)]. Future studies will need to determine where the Mn deposits in bone (e.g., trabecular, cortical, marrow) and whether it adversely affects bone structure or function. After the bone, the second highest tissue Mn concentrations in *Slc39a14*$^{-/-}$ mice were found in the brain, which also has a relatively long half-life for Mn [i.e., 52–74 d in the rat (74)]. However, unlike bone Mn concentrations, which increased over time in *Slc39a14*$^{-/-}$ mice, brain Mn concentrations decreased as the animals aged, suggestive of possible compensatory changes in brain Mn uptake/efflux. Indeed, our data showing that brain Mn accumulation in *Slc39a14*$^{-/-}$ mice was reversed by feeding a low-Mn diet indicate that Mn can be transported out of the brain in these animals.

In conclusion, our data reveal that SLC39A14 plays an essential role in Mn uptake by the liver and pancreas. Loss of hepatic SLC39A14 dramatically impairs hepatic first-pass extraction of Mn from portal blood and decreases the clearance of the metal from systemic circulation, thus resulting in diminished hepatic Mn concentrations. Impaired Mn uptake by the liver and pancreas in *Slc39a14*$^{-/-}$ mice results in reduced gastrointestinal excretion of the metal and subsequent Mn accumulation in peripheral tissues, most notably the bone and brain. Our study further reveals that one copy of *SLC39A14* may not be sufficient under conditions of Mn excess. We additionally conclude that *Slc39a14*$^{-/-}$ mice, similar to patients with loss-of-function mutations in *SLC39A14*, display motor deficits, but Mn depletion via feeding a low-Mn diet was unable to correct their motor impairments, suggesting that the deficits represent lasting effects of early-life Mn exposure. It is alternatively possible that some of the motor deficits associated with SLC39A14 deficiency are independent of brain Mn accumulation.

Methods

Animals and Diets. *Slc39a14*$^{+/-}$ mice were originally on a mixed 129 + Ter/SvJcl C57BL/6 background (52). In some studies, *Slc39a14*$^{+/-}$ mice were backcrossed for six to nine generations onto the 129S6 strain. *Slc39a14*$^{-/-}$ mice and control littermates were generated by hemizygous breeding. In our large behavioral study cohort, *Slc39a14*$^{-/-}$ mice were generated either by hemizygous breeding or by crossing hemizygous females with homozygous males. Mice were weaned at 3 wk of age, maintained on a standard chow diet (Teklad 7912; Harlan Laboratories) containing 93 ppm Mn, and housed in a 12-h light/dark cycle. In the feeding studies, mice were on a mixed background (129 + Ter/SvJcl × C57BL/6 × Balb/cJ) as used previously (37). Weanling mice were fed modified AIN-93G rodent diet formulated to contain low, normal, and high concentrations of Mn (0, 10, and 2,400 ppm Mn, respectively; Harlan Laboratories). Mn concentrations of the diets, as determined by ICP-MS, were 0.5 ppm Mn (low), 10.5 ppm Mn (normal), and 2,324 ppm Mn (high). In the large behavioral cohort, mice from the control group were fed modified AIN-93G rodent diet formulated to contain 100 ppm Mn (ResearchDiets), similar to standard chow diet (and contained 129 ppm Mn as fed). Mice in all studies were of mixed sex unless otherwise noted. Animal protocols were approved by the Institutional Animal Care and Use Committee at the University of Florida.

Measurement of Tissue Minerals. Tissue mineral concentrations were determined by using ICP-MS at the Veterinary Diagnostic Laboratory at Michigan State University.

Measurement of Tissue Mn Accumulation in Vivo. The accumulation of Mn by various tissues in vivo was measured after tail vein injection or orogastric gavage with 2 μCi [^{54}Mn]$MnCl_2$ (PerkinElmer) in sterile PBS. At the times indicated, mice were killed and whole-body and tissue ^{54}Mn-associated

radioactivity (counts per minute) were determined by using a WIZARD2 γ-counter (PerkinElmer). Tissue ^{54}Mn accumulation was calculated as a percentage of whole-body counts per minute (^{54}Mn absorbed and retained) or per gram of wet tissue. The percentage of ^{54}Mn absorbed and retained was calculated as follows: [(counts per minute in all analyzed organs − counts per minute of gastrointestinal tract) × 100/total counts per minute administered via gavage].

Measurement of Mn Excretion. Mice were administered 2 μCi [^{54}Mn]$MnCl_2$ via tail vein injection and housed individually in metabolic cages for the collection of feces/urine at the times indicated. At euthanasia, whole-body and tissue ^{54}Mn-associated counts per minute were determined as described above. Gallbladder and intestine were collected to assess gastrointestinal secretion/excretion of Mn. Radioactivity was determined for the whole intestine, the whole intestine after flushing completely with PBS, and PBS washes containing gut luminal contents.

Determination of Regional Distribution of Mn and Other Metals in Mouse Brain. Cryosections of the brain from WT and *Slc39a14*$^{-/-}$ mice at 3 wk of age were subjected to LA-ICP-MS for the determination of Mn, iron, zinc, and copper as described elsewhere (47).

Assessment of Motor Phenotype. Mice maintained on a mixed background (129 + Ter/SvJcl × C57BL/6 × Balb/cJ) were used in the main behavioral tests. The mice were bred in-house in the Animal Care facility at the University of Florida, Gainesville, and the offspring were identified by ear notching. Mice were housed in same-sex groups of two to four under standard laboratory conditions (12-h light/dark cycle, lights on at 0600 hours) with a room temperature of 22 °C and with water and food available ad libitum. All tests were performed during the light phase between 0900 and 1400 hours in accordance with the American Association for the Accreditation of Laboratory Animal Care and institutional guidelines. The Institutional Animal Care and Use Committee of the University of Florida approved the husbandry conditions of mice and all experimental protocols used in the study.

Experimental design. The mice were transferred to the behavioral laboratory at the age of ∼6 wk. Their body weight was recorded at ∼10 and ∼14 wk of age. During all experimental manipulations, the mice were handled using the hand-cupping method, since prolonged physical restraint or attempts associated with picking the mice up and restraining them by their tail increases anxiety responses in mice (75). The behavioral tests were administered sequentially when the mice were ∼11 wk of age and spanned over 4 wk. The SHIRPA overall screen was performed first, followed by the pole test, beam-traversing test, and rotarod test.

Primary neurological and sensorimotor examination. The SHIRPA screen (76) involves a series of short tests assessing the physical condition of a mouse, including the following: (*i*) body position in a cage, respiration, tremor, transfer arousal, palpebral closure, piloerection, gait, and tail elevation and (*ii*) reflexes, including pinna reflex, trunk curl, limb grasping, visual placing, negative geotaxis, and righting reflex.

Pole test. The pole test assesses motor coordination of mice descending a vertical pole (66, 77). A mouse was placed in the head-up position near the top of a vertical wooden pole (50 cm long, 1 cm in diameter, wrapped by firmly glued plastic mesh to facilitate grip and preventing sliding). The times to turn head down and descend the pole were measured by a stopwatch. The cutoff time of the test was 120 s. The average durations to turn to the head-down position and the time to descend the pole are reported.

Grip strength test. The grip strength test is widely used as a noninvasive method to evaluate mouse limb strength. It is based on the natural tendency of a mouse to grasp a bar or a grid when briefly suspended by its tail. The maximum pull-force at the time an animal released its grip was recorded on a horizontally mounted scale (Pesola Spring Scale model 40300), equipped with a drag pointer. The averaged maximum score across the two tests was used for the analysis.

Beam-traversing test. The beam-traversing test assesses a mouse's ability to maintain balance while traversing a narrow beam to reach the safety of a goal cage (64). Two types of square aluminum beams (2.5 and 1.7 cm wide, respectively; both 110 cm long) were used in the test. Both beams were fitted with 0.6-cm^2 square obstacles that were perpendicular to the width of a beam and spaced at 10-cm intervals. The beam was elevated 50 cm above the surface of a testing bench. The start end was lit by a 40-W lamp fixed ∼25 cm above the beam, while the opposite goal end was aligned with a 4.5-cm circular opening in the goal cage. Following habituation, the mice were tested during four consecutive days, traversing the wider beam during the first 2 d, followed by 2 d of traversing the narrower beam. Each day of testing comprised two trials. A fall from the beam terminated the test. The cutoff time was set to 120 s.

Rotarod test. The rotarod test evaluates neurological deficits in motor coordination in rodents (78). In this test, animals are placed on a horizontal rod that rotates along its long axis, forcing animals to walk forward to remain upright and not to fall off. The mice were trained in squads of four animals in a Rotamex-5 apparatus (Columbus Instruments). The apparatus was fitted with a mouse rod (spindle) 3 cm in diameter and was mounted 44 cm above the surface to prevent the mice from jumping off. Following habituation, mice were tested over three consecutive days, with three 5-min trials (intertrial interval of 40–50 min) and gradual acceleration of the rod from 4 to 40 rpm within 5-min trial. The time to stay on the rod was recorded by the infrared sensors. The averaged rotation speed at the fall and the time to the fall for the three trials of each session (day of testing) are reported.

Statistical Analysis. Data are shown as mean ± SEM unless indicated otherwise. Means were compared by using, where appropriate, a Student's unpaired *t* test or one-way ANOVA with Tukey's post hoc test. $P < 0.05$ was considered statistically significant. Datasets with unequal variances were log-transformed before statistical analysis. Analyses were performed by using GraphPad PRISM 5 software. For behavioral studies, departures from normal distribution were checked using the Kolmogorov–Smirnov goodness-of-fit test. A general linear model of factorial ANOVA (Statistical Package for Social Sciences, version 23; SPSS, Inc.) was used to analyze the data, with genotype as a between-subject factor and test sessions as a within-subject factor. When necessary, degrees of freedom were adjusted by Greenhouse–Geisser epsilon correction for the heterogeneity of variance. Comparisons between two independent groups were done by using Student's *t* test. Comparisons of scores obtained on an ordinal scale of measurement (SHIRPA screen) were performed using a nonparametric Mann–Whitney *U* test for two independent samples. The critical α level was set to 0.05. Due to space limitations, only significant results pertaining to the main experimental factors and interactions are reported. Also, due to smaller sample sizes in some groups and the unbalanced representation of sexes, we did not include sex as a factor in our analyses.

Detailed descriptions of siRNA experimentation and Mn uptake measurement in HepG2 cells, Western blot analyses, and the initial assessment of motor phenotype in mice are provided in *Supporting Information*.

ACKNOWLEDGMENTS. We thank Astrid Küppers [Zentralinstitut für Engineering, Elektronik, und Analytik (ZEA-3), Forschungszentrum Jülich] and Ricarda Uerlings (Institut für Molekulare Pathobiochemie, Experimentelle Gentherapie und Klinische Chemie, Rheinisch-Westfälische Technische Hochschule University Hospital Aachen) for technical help in performing the LA-ICP-MS measurements. This work was supported by NIH Grant DK080706 (to M.D.K.) and the University of Florida Research Opportunity Seed Fund (to M.D.K. and B.G.).

1. Roth J, Ponzoni S, Aschner M (2013) Manganese homeostasis and transport. *Met Ions Life Sci* 12:169–201.
2. Schroeder HA, Balassa JJ, Tipton IH (1966) Essential trace metals in man: Manganese. A study in homeostasis. *J Chronic Dis* 19:545–571.
3. O'Neal SL, et al. (2014) Manganese accumulation in bone following chronic exposure in rats: Steady-state concentration and half-life in bone. *Toxicol Lett* 229:93–100.
4. Davis CD, Zech L, Greger JL (1993) Manganese metabolism in rats: An improved methodology for assessing gut endogenous losses. *Proc Soc Exp Biol Med* 202: 103–108.
5. Myers JE, et al. (2003) Nervous system effects of occupational manganese exposure on South African manganese mineworkers. *Neurotoxicology* 24:649–656.
6. Wang D, Du X, Zheng W (2008) Alteration of saliva and serum concentrations of manganese, copper, zinc, cadmium and lead among career welders. *Toxicol Lett* 176: 40–47.
7. Lucchini R, Bergamaschi E, Smargiassi A, Festa D, Apostoli P (1997) Motor function, olfactory threshold, and hematological indices in manganese-exposed ferroalloy workers. *Environ Res* 73:175–180.
8. Bader M, Dietz MC, Ihrig A, Triebig G (1999) Biomonitoring of manganese in blood, urine and axillary hair following low-dose exposure during the manufacture of dry cell batteries. *Int Arch Occup Environ Health* 72:521–527.
9. Srivastava AK, et al. (1991) An investigation of metal concentrations in blood of industrial workers. *Vet Hum Toxicol* 33:280–282.
10. Nagatomo S, et al. (1999) Manganese intoxication during total parenteral nutrition: Report of two cases and review of the literature. *J Neurol Sci* 162:102–105.
11. Aschner JL, et al. (2015) Neuroimaging identifies increased manganese deposition in infants receiving parenteral nutrition. *Am J Clin Nutr* 102:1482–1489.
12. Butterworth RF, Spahr L, Fontaine S, Layrargues GP (1995) Manganese toxicity, dopaminergic dysfunction and hepatic encephalopathy. *Metab Brain Dis* 10:259–267.

13. Janocha-Litwin J, Marianska K, Serafinska S, Simon K (2015) Manganese encephalopathy among ephedron abusers. *J Neuroimaging* 25:832–835.
14. Aschner JL, Aschner M (2005) Nutritional aspects of manganese homeostasis. *Mol Aspects Med* 26:353–362.
15. Papavasiliou PS, Miller ST, Cotzias GC (1966) Role of liver in regulating distribution and excretion of manganese. *Am J Physiol* 211:211–216.
16. Horning KJ, Caito SW, Tipps KG, Bowman AB, Aschner M (2015) Manganese is essential for neuronal health. *Annu Rev Nutr* 35:71–108.
17. Tuschl K, et al. (2016) Syndrome of hepatic cirrhosis, dystonia, polycythemia, and hypermanganesemia caused by mutations in SLC30A10, a manganese transporter in man. *Am J Hum Genet* 99:521.
18. Quadri M, et al. (2015) Manganese transport disorder: Novel SLC30A10 mutations and early phenotypes. *Mov Disord* 30:996–1001.
19. Quadri M, et al. (2012) Mutations in SLC30A10 cause parkinsonism and dystonia with hypermanganesemia, polycythemia, and chronic liver disease. *Am J Hum Genet* 90: 467–477.
20. Hutchens S, et al. (2017) Deficiency in the manganese efflux transporter SLC30A10 induces severe hypothyroidism in mice. *J Biol Chem* 292:9760–9773.
21. Chen P, Bowman AB, Mukhopadhyay S, Aschner M (2015) SLC30A10: A novel manganese transporter. *Worm* 4:e1042648.
22. Nishito Y, et al. (2016) Direct comparison of manganese detoxification/efflux proteins and molecular characterization of ZnT10 protein as a manganese transporter. *J Biol Chem* 291:14773–14787.
23. Zogzas CE, Aschner M, Mukhopadhyay S (2016) Structural elements in the transmembrane and cytoplasmic domains of the metal transporter SLC30A10 are required for its manganese efflux activity. *J Biol Chem* 291:15940–15957.
24. Leyva-Illades D, et al. (2014) SLC30A10 is a cell surface-localized manganese efflux transporter, and parkinsonism-causing mutations block its intracellular trafficking and efflux activity. *J Neurosci* 34:14079–14095.
25. Liu C, et al. (2017) Hypothyroidism induced by loss of the manganese efflux transporter SLC30A10 may be explained by reduced thyroxine production. *J Biol Chem* 292: 16605–16615.
26. Chen P, Chakraborty S, Peres TV, Bowman AB, Aschner M (2015) Manganese-induced neurotoxicity: From C. elegans to humans. *Toxicol Res (Camb)* 4:191–202.
27. Menon AV, Chang J, Kim J (2016) Mechanisms of divalent metal toxicity in affective disorders. *Toxicology* 339:58–72.
28. Veuthey T, Wessling-Resnick M (2014) Pathophysiology of the Belgrade rat. *Front Pharmacol* 5:82.
29. Illing AC, Shawki A, Cunningham CL, Mackenzie B (2012) Substrate profile and metal-ion selectivity of human divalent metal-ion transporter-1. *J Biol Chem* 287: 30485–30496.
30. Shawki A, et al. (2015) Intestinal DMT1 is critical for iron absorption in the mouse but is not required for the absorption of copper or manganese. *Am J Physiol Gastrointest Liver Physiol* 309:G635–G647.
31. Chua AC, Morgan EH (1997) Manganese metabolism is impaired in the Belgrade laboratory rat. *J Comp Physiol B* 167:361–369.
32. Lin W, et al. (2017) Hepatic metal ion transporter ZIP8 regulates manganese homeostasis and manganese-dependent enzyme activity. *J Clin Invest* 127:2407–2417.
33. Taylor KM, Morgan HE, Johnson A, Nicholson RI (2005) Structure-function analysis of a novel member of the LIV-1 subfamily of zinc transporters, ZIP14. *FEBS Lett* 579: 427–432.
34. Liuzzi JP, Aydemir F, Nam H, Knutson MD, Cousins RJ (2006) Zip14 (Slc39a14) mediates non-transferrin-bound iron uptake into cells. *Proc Natl Acad Sci USA* 103: 13612–13617.
35. Pinilla-Tenas JJ, et al. (2011) Zip14 is a complex broad-scope metal-ion transporter whose functional properties support roles in the cellular uptake of zinc and nontransferrin-bound iron. *Am J Physiol Cell Physiol* 301:C862–C871.
36. Tuschl K, et al. (2016) Mutations in SLC39A14 disrupt manganese homeostasis and cause childhood-onset parkinsonism-dystonia. *Nat Commun* 7:11601.
37. Jenkitkasemwong S, et al. (2015) SLC39A14 is required for the development of hepatocellular iron overload in murine models of hereditary hemochromatosis. *Cell Metab* 22:138–150.
38. Hardy IJ, Gillanders L, Hardy G (2008) Is manganese an essential supplement for parenteral nutrition? *Curr Opin Clin Nutr Metab Care* 11:289–296.
39. Kato M (1963) Distribution and excretion of radiomanganese administered to mouse. *Q J Exp Physiol Cogn Med Sci* 48:355–369.
40. Greenberg DM, Copp DH, Cuthbertson EM (1943) Studies in mineral metabolism with the aid of artificial radioactive isotopes: VII. The distribution and excretion, particularly by way of the bile, of iron, cobalt, and manganese. *J Biol Chem* 147:749–756.
41. Schramm VL, Brandt M (1986) The manganese(II) economy of rat hepatocytes. *Fed Proc* 45:2817–2820.
42. Finley JW (1998) Manganese uptake and release by cultured human hepatocarcinoma (Hep-G2) cells. *Biol Trace Elem Res* 64:101–118.
43. Davidsson L, Lönnerdal B, Sandström B, Kunz C, Keen CL (1989) Identification of transferrin as the major plasma carrier protein for manganese introduced orally or intravenously or after in vitro addition in the rat. *J Nutr* 119:1461–1464.
44. Nam H, et al. (2013) ZIP14 and DMT1 in the liver, pancreas, and heart are differentially regulated by iron deficiency and overload: Implications for tissue iron uptake in iron-related disorders. *Haematologica* 98:1049–1057.
45. Zheng W, Kim H, Zhao Q (2000) Comparative toxicokinetics of manganese chloride and methylcyclopentadienyl manganese tricarbonyl (MMT) in Sprague-Dawley rats. *Toxicol Sci* 54:295–301.
46. Meyer LA, Durley AP, Prohaska JR, Harris ZL (2001) Copper transport and metabolism are normal in aceruloplasminemic mice. *J Biol Chem* 276:36857–36861.
47. Boaru SG, et al. (2014) Simultaneous monitoring of cerebral metal accumulation in an experimental model of Wilson's disease by laser ablation inductively coupled plasma mass spectrometry. *BMC Neurosci* 15:98.
48. Sato I, Matsusaka N, Kobayashi H, Nishimura Y (1996) Effects of dietary manganese contents on 54Mn metabolism in mice. *J Radiat Res (Tokyo)* 37:125–132.
49. Keen CL, Bell JG, Lönnerdal B (1986) The effect of age on manganese uptake and retention from milk and infant formulas in rats. *J Nutr* 116:395–402.
50. Tucker LB, Fu AH, McCabe JT (2016) Performance of male and female C57BL/6J mice on motor and cognitive tasks commonly used in pre-clinical traumatic brain injury research. *J Neurotrauma* 33:880–894.
51. Kovács AD, Pearce DA (2013) Location- and sex-specific differences in weight and motor coordination in two commonly used mouse strains. *Sci Rep* 3:2116.
52. Hojyo S, et al. (2011) The zinc transporter SLC39A14/ZIP14 controls G-protein coupled receptor-mediated signaling required for systemic growth. *PLoS One* 6:e18059.
53. Aydemir TB, et al. (2012) Zinc transporter ZIP14 functions in hepatic zinc, iron and glucose homeostasis during the innate immune response (endotoxemia). *PLoS One* 7: e48679.
54. Aydemir TB, Sitren HS, Cousins RJ (2012) The zinc transporter Zip14 influences c-Met phosphorylation and hepatocyte proliferation during liver regeneration in mice. *Gastroenterology* 142:1536–1546.e5.
55. Wessels I, Cousins RJ (2015) Zinc dyshomeostasis during polymicrobial sepsis in mice involves zinc transporter Zip14 and can be overcome by zinc supplementation. *Am J Physiol Gastrointest Liver Physiol* 309:G768–G778.
56. Aydemir TB, et al. (2017) Metal transporter Zip14 (Slc39a14) deletion in mice increases manganese deposition and produces neurotoxic signatures and diminished motor activity. *J Neurosci* 37:5996–6006.
57. Xin Y, et al. (2017) Manganese transporter Slc39a14 deficiency revealed its key role in maintaining manganese homeostasis in mice. *Cell Discov* 3:17025.
58. Gibbons RA, et al. (1976) Manganese metabolism in cows and goats. *Biochim Biophys Acta* 444:1–10.
59. Bertinchamps AJ, Miller ST, Cotzias GC (1966) Interdependence of routes excreting manganese. *Am J Physiol* 211:217–224.
60. Cotzias GC, Papavasiliou PS (1964) Primordial homeostasis in a mammal as shown by the control of manganese. *Nature* 201:828–829.
61. Dydak U, et al. (2011) In vivo measurement of brain GABA concentrations by magnetic resonance spectroscopy in smelters occupationally exposed to manganese. *Environ Health Perspect* 119:219–224.
62. Fitsanakis VA, et al. (2006) The use of magnetic resonance imaging (MRI) in the study of manganese neurotoxicity. *Neurotoxicology* 27:798–806.
63. Racette BA (2014) Manganism in the 21st century: The Hanninen lecture. *Neurotoxicology* 45:201–207.
64. Carter RJ, et al. (1999) Characterization of progressive motor deficits in mice transgenic for the human Huntington's disease mutation. *J Neurosci* 19:3248–3257.
65. Chesselet MF, Carmichael ST (2012) Animal models of neurological disorders. *Neurotherapeutics* 9:241–244.
66. Chesselet MF, et al. (2012) A progressive mouse model of Parkinson's disease: The Thy1-aSyn ("Line 61") mice. *Neurotherapeutics* 9:297–314.
67. Janus C, Hernandez C, deLelys V, Roder H, Welzl H (2016) Better utilization of mouse models of neurodegenerative diseases in preclinical studies: From the bench to the clinic. *Methods Mol Biol* 1438:311–347.
68. Lalonde R, Dumont M, Staufenbiel M, Sturchler-Pierrat C, Strazielle C (2002) Spatial learning, exploration, anxiety, and motor coordination in female APP23 transgenic mice with the Swedish mutation. *Brain Res* 956:36–44.
69. Schindowski K, et al. (2006) Alzheimer's disease-like tau neuropathology leads to memory deficits and loss of functional synapses in a novel mutated tau transgenic mouse without any motor deficits. *Am J Pathol* 169:599–616.
70. Brooks SP, Dunnett SB (2009) Tests to assess motor phenotype in mice: A user's guide. *Nat Rev Neurosci* 10:519–529.
71. Roth JA (2014) Correlation between the biochemical pathways altered by mutated Parkinson-related genes and chronic exposure to manganese. *Neurotoxicology* 44: 314–325.
72. Herrero Hernandez E, et al. (2006) Follow-up of patients affected by manganese-induced parkinsonism after treatment with CaNa2EDTA. *Neurotoxicology* 27: 333–339.
73. Peres TV, et al. (2015) Developmental exposure to manganese induces lasting motor and cognitive impairment in rats. *Neurotoxicology* 50:28–37.
74. Takeda A, Sawashita J, Okada S (1995) Biological half-lives of zinc and manganese in rat brain. *Brain Res* 695:53–58.
75. Hurst JL, West RS (2010) Taming anxiety in laboratory mice. *Nat Methods* 7:825–826.
76. Rogers DC, et al. (1997) Behavioral and functional analysis of mouse phenotype: SHIRPA, a proposed protocol for comprehensive phenotype assessment. *Mamm Genome* 8:711–713.
77. Fleming SM, et al. (2004) Early and progressive sensorimotor anomalies in mice overexpressing wild-type human alpha-synuclein. *J Neurosci* 24:9434–9440.
78. Dunham NW, Miya TS (1957) A note on a simple apparatus for detecting neurological deficit in rats and mice. *J Am Pharm Assoc Am Pharm Assoc* 46:208–209.